

# Rapid determination of $^{230}\text{Th}$ and $^{231}\text{Pa}$ in seawater by desolvated micro-nebulization Inductively Coupled Plasma magnetic sector mass spectrometry

M.S. Choi <sup>a,b</sup>, R. Francois <sup>b,\*</sup>, K. Sims <sup>c</sup>, M.P. Bacon <sup>b</sup>, S. Brown-Leger <sup>b</sup>,  
A.P. Fler <sup>b</sup>, L. Ball <sup>b</sup>, D. Schneider <sup>b</sup>, S. Pichat <sup>d</sup>

<sup>a</sup> Isotope Research Team, Korea Basic Science Institute, Taejeon 305-333, South Korea

<sup>b</sup> Department of Marine Chemistry and Geochemistry, Woods Hole Oceanographic Institution, Woods Hole, MA 02543, USA

<sup>c</sup> Department of Geology and Geophysics, Woods Hole Oceanographic Institution, Woods Hole, MA 02543, USA

<sup>d</sup> Laboratoire des Sciences de la Terre, Ecole Normale Supérieure de Lyon, Lyon, F-69364, France

Received 16 November 2000; received in revised form 6 June 2001; accepted 15 June 2001

## Abstract

Difficulties in determining the  $^{230}\text{Th}$  and  $^{231}\text{Pa}$  concentration of seawater have hindered rapid progress in the application of these unique natural tracers of particle scavenging and ocean circulation. In response, we have developed an ICP/MS analytical procedure combining a degree of sensitivity, precision and sample throughput that can facilitate the systematic measurement of basin-scale changes in  $^{230}\text{Th}$  and  $^{231}\text{Pa}$  seawater concentration, and provide important constraints on circulation and mixing rates in the deep ocean.

Seawater samples are spiked with  $^{229}\text{Th}$  and  $^{233}\text{Pa}$  and equilibrated before pre-concentration using conventional methods of Fe oxyhydroxide co-precipitation and anion exchange. Isotopic ratios are measured using a Finnigan MAT Element magnetic sector Inductively Coupled Plasma mass spectrometer (ICP/MS) equipped with a desolvating micronebulizer. Measurements are done on 10–20 l seawater samples with an internal precision of  $\sim 2\%$  and a reproducibility of  $\sim 5\%$  (95% confidence intervals (CI)) in deep water. After correction for procedural blank,  $^{232}\text{Th}$  tailing, and  $^{232}\text{Th}^1\text{H}$  interference, the detection limits are  $\sim 3$  fg for  $^{230}\text{Th}$  and  $\sim 0.4$  fg for  $^{231}\text{Pa}$ . Applied to 20 l volumes, these detection limits correspond to concentrations of 0.15 fg/kg for  $^{230}\text{Th}$  and 0.02 fg/kg for  $^{231}\text{Pa}$ , which are 5–15 times lower than typical concentrations in surface water. The capability of this method is illustrated by two seawater profiles from the Equatorial Atlantic region that show systematic variations in  $^{230}\text{Th}$  and  $^{231}\text{Pa}$  concentration consistent with patterns of deep water circulation. © 2001 Elsevier Science B.V. All rights reserved.

**Keywords:**  $^{230}\text{Th}$ ;  $^{231}\text{Pa}$ ; Seawater; ICP/MS

## 1. Introduction

$^{230}\text{Th}$  ( $t_{1/2} = 75,690$  years) and  $^{231}\text{Pa}$  ( $t_{1/2} = 32,760$  years) are produced uniformly in seawater from radioactive decay of  $^{238}\text{U}$  and  $^{235}\text{U}$ . Both are

\* Corresponding author. Tel.: +1-508-289-2637; fax: +1-508-457-2193.

E-mail address: rfrancois@whoi.edu (R. Francois).

rapidly adsorbed on settling particles and removed into the sediment, but differ slightly in their affinity for particles, with  $^{230}\text{Th}$  being more rapidly removed from seawater. These characteristics (well-constrained source, high but slightly different particle reactivity) have led to a wide range of applications as tracers of particle scavenging (Nozaki et al., 1981; Bacon and Anderson, 1982; Bacon, 1988; Cochran, 1992; Luo et al., 1995; Edmonds et al., 1998), particle rain rate (Bacon, 1984; Francois et al., 1990), sediment focusing and winnowing (Suman and Bacon, 1989; Francois et al., 1993; Frank et al., 1999), paleo-productivity (Lao et al., 1992; Kumar et al., 1993; Francois et al., 1997; Walter et al., 1999) and deep water circulation in the modern ocean (Rutgers van der Loeff and Berger, 1993; Scholten et al., 1995; Moran et al., 1997; Vogler et al., 1998; Francois et al., 2000) and ancient oceans (Yu et al., 1996; Marchal et al., 2000).

In order to fully realize the potential of these approaches, however, an extensive and precise database on the distribution of the two radionuclides in seawater is required (Henderson et al., 1999; Marchal et al., 2000). Because of the very low concentration of  $^{230}\text{Th}$  and  $^{231}\text{Pa}$  in seawater (typically 0.05–1 dpm/m<sup>3</sup> or 0.5–30 fg/kg), developing such a database has proven difficult. Earlier measurements were made by  $\alpha$ -spectrometry, which required processing very large volumes of seawater (m<sup>3</sup>) and elaborate wet chemistry (Anderson and Fleer, 1982; Nozaki and Nakanishi, 1985; Nozaki et al., 1987; Fleer and Bacon, 1991; Buesseler et al., 1992; Rutgers van der Loeff and Berger, 1993; Scholten et al., 1995). This method resulted in relatively low precision (typically 5–10%) and sample coverage. Precise  $^{231}\text{Pa}$  measurements were particularly difficult because the yield monitor,  $^{233}\text{Pa}$ , is a  $\beta$ -emitter, thus preventing the direct counting of  $^{231}\text{Pa}/^{233}\text{Pa}$  ratios and requiring the accurate evaluation of the efficiency of the  $\alpha$  and  $\beta$  counters. More recently, several  $^{230}\text{Th}$  (Moran et al., 1995, 1997; Vogler et al., 1998) and  $^{231}\text{Pa}$  (Edmonds et al., 1998) seawater profiles have been measured by isotope dilution using Thermal Ionization Mass Spectrometry (TIMS). This method is much more sensitive, allowing the measurement of the two radionuclides on a few liters of seawater with good precision (2–3%). However, the need for rigorous matrix sepa-

ration, highly specialized analytical equipment, and difficult sample loading severely limit sample throughput. An additional complication for  $^{231}\text{Pa}$  is that the only isotope available for addition to the samples is the short-lived  $^{233}\text{Pa}$  ( $t_{1/2} = 26.967$  days), which requires immediate measurement after preparation of the sample (Pickett et al., 1994; Edmonds et al., 1998; Bourdon et al., 1999).

Here, we report an Inductively Coupled Plasma mass spectrometry (ICP/MS) method that combines high sample throughput with sensitivity and precision approaching those attainable by TIMS. Inductively Coupled Plasma mass spectrometers are versatile instruments that have rapidly become the tool of choice for many ultra-trace analyses. They require only a few minutes for data acquisition, and their continuously improving sensitivity is now reaching  $\sim 5 \times 10^9$  cps/ppm in the transuranic atomic mass range when samples are introduced into the plasma with a desolvating micronebulizer (sample aspiration rate  $\sim 100 \mu\text{l}/\text{min}$ ). In addition to high sensitivity, sector-type ICP/MS's also have negligible background counts, which contribute to lowering detection limits below the fg/g level (Field and Sherrell, 1998; Eroglu et al., 1998). Seawater  $^{230}\text{Th}$  and  $^{231}\text{Pa}$  can thus be rapidly analyzed on 10–20 l samples with a precision of 1–5%. While these volumes are somewhat larger than required by TIMS, adequate samples can still be readily obtained by hydrocasts, and the higher sample throughput and ubiquity of the ICP mass spectrometers should enable the rapid expansion of the database and the detailed study of the distribution and control of the concentration of  $^{230}\text{Th}$  and  $^{231}\text{Pa}$  in seawater on basin-wide scales.

## 2. Experimental

### 2.1. Sampling procedure

The seawater samples (15–20 l) were immediately drained (for total concentration) or filtered gravitationally (for dissolved concentration) from the hydrocast bottles into 20 l polyethylene collapsible cubitainers and weighed with a precision better than 1% on a computerized balance that averages out the accelerations from the ship's motion. The samples were then acidified with 30 ml 6 N HCl and spiked

with  $^{229}\text{Th}$ ,  $^{233}\text{Pa}$ , and 1 ml  $\text{FeCl}_3$  (50 mg/ml; cleaned by extraction in isopropyl ether). After a period of at least 12 h for equilibration, the pH was adjusted to  $\sim 8.5$ – $9$  by adding  $\sim 17$  ml of  $\text{NH}_4\text{OH}$  (conc.) to precipitate Fe oxyhydroxides that adsorb dissolved and entrain particulate Th and Pa. The resulting precipitate was decanted slowly, first to the bottom of the cubitainers, from which most of the overlying water was removed. When the volume of water was reduced to  $\sim 1$  l, the suspension was transferred to a 1-l plastic beaker to continue decantation until the residual water was reduced to  $\sim 100$ – $200$  ml. Thereupon, the precipitate was centrifuged in 50-ml polypropylene centrifuge tubes and returned to the laboratory for analysis.

## 2.2. Sample preparation

Th, Pa and U were separated by anion exchange on AG1-X8 resin (100–200 mesh) by a procedure that was modified after the method described by Fleer and Bacon (1991) and optimized by tracer experiments with  $^{234}\text{Th}$  and  $^{233}\text{Pa}$ . The samples were first redissolved in 9 N HCl by adding a volume (typically  $\sim 10$ – $20$  ml) of concentrated HCl (12 N) equivalent to three times the volume of Fe oxyhydroxide recovered by decantation and centrifugation. A  $\sim 4$  ml column of AG1-X8 resin packed into a  $0.6 \times 20$  cm polyethylene tube with a polyethylene frit (KONTES™) was pre-conditioned with HCl 9 N. The dissolved sample was passed through the column and rinsed with an additional 12 ml of 9 N HCl. The Th fraction, which is not retained by the resin, was collected in a Teflon™ beaker. The Pa fraction, which is adsorbed on the chloride column with Fe and U, was eluted into a separate Teflon beaker with 12 ml of 9 N HCl plus 0.14 N HF. The U and Fe that remain on the column were discarded. The Th fraction was then evaporated to a small volume and taken up in 8 N  $\text{HNO}_3$  to be further purified by elution through a second anion-exchange column of AG1-X8 pre-conditioned with 8 N  $\text{HNO}_3$ . The eluted Pa fraction was spiked with  $^{236}\text{U}$  ( $\sim 70$  pg), equilibrated overnight and passed through another AG1-X8 column pre-conditioned with 9 N HCl. The column was further eluted with 12 ml of 9 N HCl plus 0.14 N HF and the total eluate recovered in the Teflon™ beaker. The purpose of adding  $^{236}\text{U}$  prior to the last

column for Pa is to check for possible  $^{233}\text{U}$  “bleeding” in the final Pa fraction.  $^{233}\text{U}$  is produced by decay of  $^{233}\text{Pa}$  and the two isotopes cannot be distinguished by ICP/MS. Since  $^{231}\text{Pa}$  is quantified from the  $^{231}\text{Pa}/^{233}\text{Pa}$  ratio measured in the Pa eluate, any U “bleeding” would add  $^{233}\text{U}$  to the solution and interfere with the measurements. Adding  $^{236}\text{U}$  prior to the last Pa column provides a means of quantifying possible U contribution to the 233 atomic mass unit peak. If significant  $^{236}\text{U}$  is found in the last Pa eluate, U can in turn be eluted from the last column with 1 N HCl and its  $^{233}\text{U}/^{236}\text{U}$  measured to correct for the presence of  $^{233}\text{U}$  in the Pa fraction. In our experience, however, this is very rarely required as the column separation of U and Pa is very efficient (typically,  $< 0.01\%$  of the added  $^{236}\text{U}$  passes through the column) and most of the  $^{233}\text{U}$  has already been removed on the first chloride column. After elution, the Th and Pa solutions were each reduced to a drop in a small screw-cap Teflon™ vial. Just prior to analysis, 0.3 ml of Milli-Q water was added to the Th fraction. For the Pa fraction, 0.3 ml of 1 N  $\text{HNO}_3$  plus 0.14 N HF was added and the closed vial heated to  $60^\circ\text{C}$  in a drying oven overnight in order to prevent the loss of hydrolyzed Pa complexes on the walls of the vial. The resulting solutions were then filtered through acid-washed Acrodisk™ filters (0.2  $\mu\text{m}$  pore size) to prevent clogging of the micronebulizer. High purity acids (HCl,  $\text{HNO}_3$  and HF; Seastar™) were used throughout the procedure, and all Teflonware and resins were thoroughly acid-cleaned.

During the  $^{234}\text{Th}$  and  $^{233}\text{Pa}$  tracer experiments, column recoveries were 100% ( $\pm 10\%$ ), and cross-contamination between Th and Pa  $< 1\%$ .

Overall recoveries were typically 50–70% for both isotopes. Most of the loss occurs during the decantation steps, and thus collection of precipitates by large volume or continuous centrifugation could improve recovery and further reduce the volume of seawater needed.

## 2.3. Sample analysis

$^{230}\text{Th}$  and  $^{231}\text{Pa}$  concentrations were calculated from the  $^{230}\text{Th}/^{229}\text{Th}$  and  $^{231}\text{Pa}/^{233}\text{Pa}$  (Pa; U) ratios measured on a magnetic sector ICP/MS (Finnigan MAT Element) in low-resolution mode (mass resolv-

ing power  $\Delta M/M = 300$ ). Samples were introduced into the plasma through a membrane desolvator (MCN-6000, Cetac Technologies) equipped with a PFA microconcentric nebulizer and a PFA spray chamber (Elemental Scientific). Passive aspiration was used to improve the stability of the ion beam and eliminate possible memory effects from the PVC tubing of the peristaltic pump. Combining the MCN-6000 and PFA microconcentric nebulizer significantly reduces the sample uptake rate ( $\sim 100 \mu\text{l}/\text{min}$ ), improves sensitivity 10-fold over standard pneumatic nebulization ( $\sim 3 \times 10^9 \text{ cps}/\text{ppm Th}$ ) without increasing background counts, and result in an overall efficiency (ions detected/atoms introduced) comparable to TIMS ( $\sim 1\%$ ). Measurements were made in the electrostatic scanning mode (i.e. by changing the acceleration voltage; Table 1) over a range of masses (229, 230, 230.5 and 231.5 for Th analysis; 231, 231.5, 233 and 236 for Pa analysis; Fig. 1). The width of each scanned peak was adjusted to clearly record the flat top area and maximize precision. Data acquisition time was  $\sim 2\text{--}3 \text{ min}$  for each fraction. To minimize carry-over between samples, the system was cleaned using an ultra-pure diluted nitric acid solution containing traces of HF after each sample run. Prior to each measurement, acid blanks were measured to quantify and correct for carry-over between samples, which was typically 1–3 cps.

## 2.4. Spikes and standards

$^{229}\text{Th}$  and  $^{233}\text{Pa}$  spikes were used for the quantification of  $^{230}\text{Th}$  and  $^{231}\text{Pa}$ , respectively. The  $^{229}\text{Th}$  solution has been calibrated by ICP/MS and TIMS against a gravimetric  $^{232}\text{Th}$  standard.  $^{233}\text{Pa}$  was produced by neutron activation of  $^{232}\text{Th}$  and purified by anion-exchange on AG1-X8 resin (Anderson and Fleer, 1982). A  $^{233}\text{Pa}$  solution has been calibrated by analyzing a dissolved sample of Table Mountain Lattite (TML), a widely used rock standard in which  $^{235}\text{U}$  and  $^{231}\text{Pa}$  are known to be in secular equilibrium. The  $^{235}\text{U}$  concentration in the rock solution was measured by isotope dilution ICP/MS using a  $^{236}\text{U}$  spike calibrated against a U gravimetric standard. The  $^{231}\text{Pa}$  concentration of the TML solution was then calculated based on  $^{235}\text{U}\text{--}^{231}\text{Pa}$  secular equilibrium and used to calibrate our  $^{233}\text{Pa}$  spike.

We also used TML to check our  $^{229}\text{Th}$  and  $^{236}\text{U}$  spike calibrations as  $^{238}\text{U}$  and  $^{230}\text{Th}$  are also in radioactive equilibrium in TML. We measured the  $^{230}\text{Th}/^{232}\text{Th}$  in a TML solution by secondary ionization mass spectrometry (Layne and Sims, 2000) and its  $^{232}\text{Th}$  and  $^{238}\text{U}$  concentrations by ICP/MS using our  $^{229}\text{Th}$  and  $^{236}\text{U}$  spikes. From these measurements, we calculated the  $^{230}\text{Th}/^{238}\text{U}$  in the TML solution. In all our measurements, the measured activity ratio of  $^{230}\text{Th}/^{238}\text{U}$  equaled unity within the uncertainty of our measurements ( $\pm 1\%$ ).

Table 1  
Typical operating parameters of sector type ICP/MS

Instrument parameters			Scanning parameters			
			Isotopes	Scanned mass range	Sample time (ms)	Samples per peak
Power, W		1350	$^{229}\text{Th}$	228.92–229.15	2	100
Gas, l/min	Cool	13.3	$^{230}\text{Th}$	229.80–230.26	2	100
	Auxiliary	1.10		230.39–230.62	2	50
	Sample	1.22		231.47–231.53	2	50
	MCN-6000		$^{231}\text{Pa}$	230.90–231.20	2	100
	Sweep	3.26		231.47–231.53	2	50
Lenses, V	$\text{N}_2$ , ml/min	14	$^{233}(\text{Pa,U})$	232.90–233.20	2	100
	Extraction	–2000	$^{236}\text{U}$	235.91–236.20	2	100
	Focus	–951				
	X-Deflector	4.6				
	Shape	89.3				
	Y-Deflector	–6.2				

Standard solutions of  $^{230}\text{Th}$  and  $^{231}\text{Pa}$  were calibrated by ICP/MS against the  $^{229}\text{Th}$  and decay-corrected  $^{233}\text{Pa}$  solutions. Isotope fractionation during ICP/MS analysis was estimated at 0.5% per amu, based on replicate measurements of the  $^{235}\text{U}/^{238}\text{U}$  of a U standard (NBS 960).

### 2.5. Samples

Several approaches were used to evaluate the performance of the method. First, thirteen samples of coastal water were filtered through 142 mm (diameter) membrane filters (0.45  $\mu\text{m}$ ) into 20 l cubitainers. They were subsequently spiked with precisely weighed aliquots of  $^{230}\text{Th}$  and  $^{231}\text{Pa}$  standard solutions to reflect the range of concentration typically found in the open ocean. These samples were then treated as unknowns following the procedure described above. To further evaluate the precision of the method, sets of replicate seawater samples were collected in the eastern tropical Atlantic. Ten  $\sim$  20-l samples were collected at 14°27.05'N and 21°54.20' W (St. J), at 2000 m depth. The 10 samples were filtered gravitationally into 10 cubitainers. Five samples were immediately weighed, acidified and spiked on board and processed as regular samples following the procedure described above. The five others were brought back to the laboratory, weighed, spiked, acidified and processed after  $\sim$  15 months storage. Two additional sets of five unfiltered samples were taken from surface (30 m) and deep (1500 m) water at 18°27.9'N and 21°01.6' W (St. M). These samples were immediately acidified with 30 ml of 6 M HCl, but stored for about 15 months before spiking and analysis. One deep (1500 m) water sample was also stored without acid.

## 3. Results and discussion

### 3.1. Spectra obtained by sector type ICP/MS

Fig. 1 shows the ICP/MS spectra for Th and Pa obtained for one of the seawater samples collected from 1500 m at station M. Peak intensity for both  $^{230}\text{Th}$  ( $\sim$  2000 cps) and  $^{231}\text{Pa}$  ( $\sim$  800 cps) is well above background (typically 1–3 cps, mainly due to carry-over between samples and some contribution

from dark noise), suggesting that sample size could be further reduced, at least below 1000 m depth, where the concentrations of the two nuclides are highest. Magnetic sector type ICP/MS produces peaks with flatter tops than quadrupole ICP/MS, which improves the precision of the measurements.

### 3.2. Corrections for $^{232}\text{Th}$ interference due to peak tailing and hydride formation

Counts obtained on masses 230, 231 and 233 have to be corrected for tailing from  $^{232}\text{Th}$ .  $^{230}\text{Th}$  has been measured in soil and deep sea sediment samples with quadrupole or sector type ICP/MS (Shaw and Francois, 1991; Hinrichs and Schnetger, 1999). For these measurements, abundance sensitivity is critical due to the predominance of  $^{232}\text{Th}$  in the samples. For seawater, Fig. 1 indicates that tailing correction is less significant. The highest  $^{232}\text{Th}/^{230}\text{Th}$  atom ratios are found in surface waters, where they can reach  $10^5$ , but at depth  $^{232}\text{Th}/^{230}\text{Th}$  ratios are generally  $10^4$  or lower. Sector type ICP/MS has abundance sensitivity of  $\sim$  5 ppm for masses 1 amu apart and  $\sim$  0.5 ppm for masses 2 amu apart. Tailing corrections on the  $^{230}\text{Th}$  peaks are thus usually  $<$  5% and often  $<$  1%. Although the  $^{231}\text{Pa}$  peak is within 1 amu of  $^{232}\text{Th}$ , tailing correction is minimized by efficient column separation of the two elements. With  $<$  1% of the Th fraction “bleeding” into the Pa solution, tail corrections on  $^{231}\text{Pa}$  are also typically  $<$  5%.

For  $^{233}\text{Pa}$  (Pa;U), isobaric interference from hydride  $^{232}\text{Th}^1\text{H}$  must also be considered (Crain and Alvarado, 1994). The mode and rate of sample introduction into the plasma are the most important factors affecting hydride generation (Crain and Alvarado, 1994; Minnich and Houk, 1998; Becker et al., 1999). With standard pneumatic nebulizers,  $^{232}\text{Th}^1\text{H}$  can be as high as 0.01% of the  $^{232}\text{Th}$  peak (Hallenbach et al., 1994). Membrane desolvation and the small sample uptake rates afforded by microcentric nebulizers minimize the generation of  $^{232}\text{Th}^1\text{H}$ . For instance, using a MCN-6000 (Cetac™), Kim et al. (2000) found that hydride formation during U analysis was reduced 7-fold ( $^{238}\text{U}^1\text{H}/^{238}\text{U} = 1.4 \times 10^{-5}$ ).

In order to quantify  $^{232}\text{Th}$  tailing and  $^{232}\text{Th}^1\text{H}$  generation, serially diluted  $^{232}\text{Th}$  standard solutions

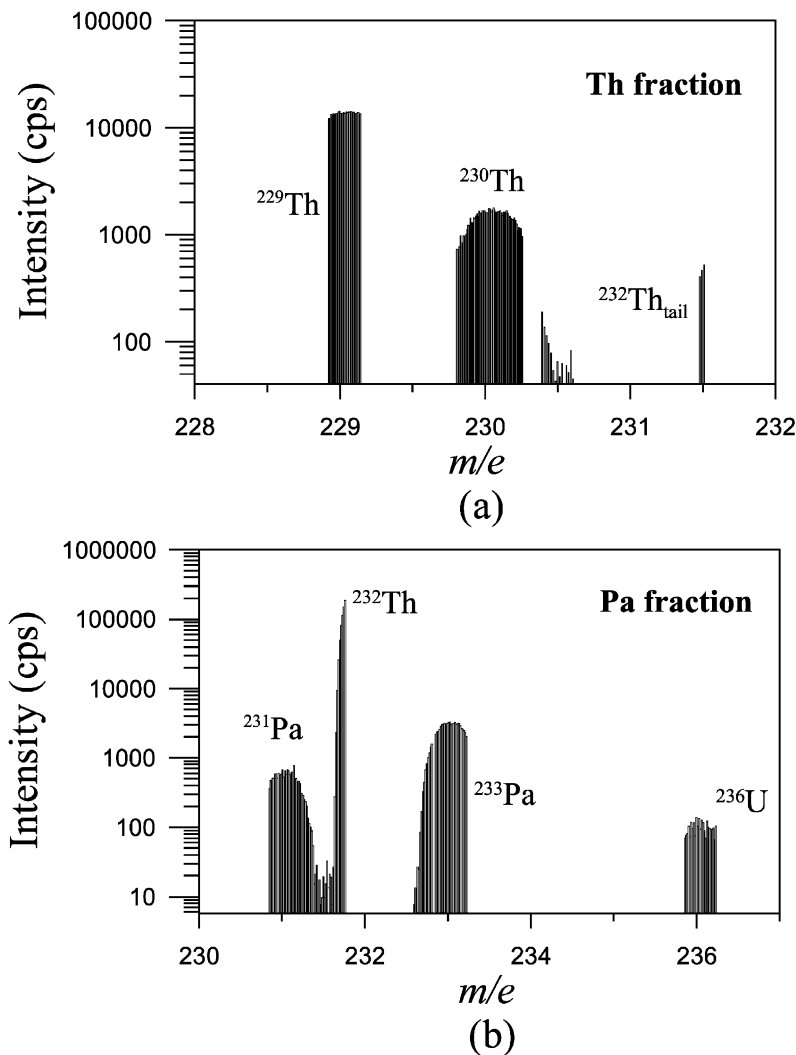


Fig. 1. Sector type ICP/MS spectra for Th (a) and Pa (b) obtained from seawater collected in the eastern Atlantic (St. M) at 1500 m. Concentrations are calculated by selecting only the channels corresponding to the top of the peaks after exporting the raw data into an Excel™ spreadsheet, and subtracting isobaric interferences from the  $^{232}\text{Th}$  tail estimated from the counts measured at mass 231.5 and the count ratios reported in Table 2.

(SPEX™ Certified Standard) were run and measured over the 230–233 mass range. Considering the concentration range of  $^{232}\text{Th}$  in seawater (4–400 pg/kg; Cochran, 1992) and the pre-concentration factor of our analytical procedure, the expected  $^{232}\text{Th}$  concentration in the final Th solution introduced into the ICP/MS is about 0.2–20 ng/ml. Since Pa is chromatographically separated from Th with an efficiency typically > 99%,  $^{232}\text{Th}$  concentration in the

final Pa fraction should be < 0.2 ng/ml. However,  $^{232}\text{Th}$  contamination, particularly from the resin, can increase  $^{232}\text{Th}$  concentration in the Pa fraction.

Table 2 shows the count rates obtained on the 230–233 mass range for  $^{232}\text{Th}$  concentrations ranging from 0.2 to 5 ng/ml. The absence of discernable peaks at mass 230 and 231 indicates that count rates on these masses come from the tailing of  $^{232}\text{Th}$ ; count rates at mass 233 combine the effect of tailing

Table 2  
Interference and peak tailing by  $^{232}\text{Th}$  in both Th and Pa fraction

$^{232}\text{Th}$ (ng/ml)	Mass number							Ratios		
	230	230.5	231	231.5	232	232.5	233	230/231.5	231/231.5	233/231.5
0.2	< 1 <sup>a</sup>	2	5	16	$0.85 \times 10^6$	62	8	–	0.32	0.50
0.5	< 1	6	13	39	$2.3 \times 10^6$	157	19	–	0.32	0.48
1	2	11	25	83	$(4.4 \times 10^6)^b$	276	43	0.024	0.31	0.52
5	12	50	141	411	$(23 \times 10^6)^b$	1478	221	0.029	0.34	0.54

<sup>a</sup>Count per second (cps).

<sup>b</sup>Extrapolated from count rates for lower concentrations.

and ThH formation. The average 233/232 ratio is  $0.95 \times 10^{-5}$ , which is comparable to  $0.95 \times 10^{-5}$  (Eroglu et al., 1998) and  $1.4 \times 10^{-5}$  measured for UH (Kim et al., 2000), and lower than  $2.1 \times 10^{-5}$  (Crain and Alvarado, 1994) and  $2.7 \times 10^{-5}$  (Minich and Houk, 1998) measured for ThH. Because over-ranging occurs on the 232 peak when  $^{232}\text{Th}$  concentration exceeds 0.5 ng/ml, tailing intensity was also measured at 230.5, 231.5, and 232.5, and count rates at 231.5 were used as reference to estimate  $^{232}\text{Th}$  interferences on the 230, 231 and 233 masses. The ratios 230/231.5, 231/231.5 and 233/231.5 are 0.03, 0.3 and 0.5, respectively. In the example shown in Fig. 1, count rates at 231.5 was 400 cps in the Th fraction and 10 cps in the Pa fraction. The resulting  $^{232}\text{Th}$  interference corrections were 12 cps on 230 (0.6% of the 230 peak intensity), 3 cps on 231 (0.4% of the 231 peak intensity) and 5 cps on 233 (0.2% 233 peak intensity). Similar corrections were applied to all the samples and blanks. Corrections in surface waters can be ~10 times higher due to their higher  $^{232}\text{Th}/^{230}\text{Th}$  ratios. The Pa spectrum also shows a peak at mass 236 (~100 cps: ~6 fg  $^{236}\text{U}$ ), which indicates negligible U bleeding (< 0.01%) in the Pa fraction.

### 3.3. Isotopic fractionation and stability of isotopic ratios during analysis

Analytical errors may also arise as a result of variable isotopic fractionation during ICP/MS measurements (Heumann et al., 1998; Catterick et al., 1998). Two monitor solutions produced by combining calibrated Th (11.5 pg/g  $^{230}\text{Th}$  plus 8.6 pg/g  $^{229}\text{Th}$ ) and Pa (0.2 pg/g  $^{231}\text{Pa}$  plus 1.2 pg/g  $^{233}\text{Pa}$ ) standard solutions were analyzed repeatedly to check

the short-term and long-term variability of isotopic ratio measurements (Fig. 2). Based on replicate measurements of NBS 960 uranium standard, which has a natural  $^{238}\text{U}/^{235}\text{U}$  ratio (137.88), a mass fractionation factor of 0.5%/amu was applied to the expected Th and Pa isotopic ratios. The mass fractionation correction based upon  $^{235}\text{U}/^{238}\text{U}$  of NBS 960 can vary by ~0.1% within a day (Sims et al., submitted for publication), which is much smaller than the uncertainties in our measurements. The long-term variability in the measured isotopic ratios was similar to the precision of measurement of individual ratios, ~1% (2 se) for the Th monitor, and ~3% (2 se) for the Pa monitor. Isotopic fractionation and its long-term variability are thus within the precision to which typical seawater samples can be measured.

### 3.4. Decay of $^{233}\text{Pa}$ to $^{233}\text{U}$ and implications for $^{231}\text{Pa}$ measurements

Short-lived  $^{233}\text{Pa}$  decays to long-lived ( $t_{1/2} = 159,200$  years)  $^{233}\text{U}$ . The Pa monitor was initially prepared from a  $^{233}\text{Pa}$  solution that had just been eluted from a HCl(9 N)-conditioned AG1-X8 column twice to remove  $^{233}\text{U}$ . Its  $^{231}\text{Pa}/^{233}(\text{Pa} + \text{U})$  ratio was monitored over a period of 45 days, during which its  $^{233}\text{U}/^{233}\text{Pa}$  rose from 0 to 2.2. Notwithstanding this change in elemental composition, the  $^{231}\text{Pa}/^{233}(\text{Pa} + \text{U})$  ratio remained within the precision of the analysis (Fig. 2). This observation indicates that ICP/MS's do not differentiate between  $^{233}\text{U}$  and  $^{233}\text{Pa}$ . This is in contrast to thermal ionization, during which U ionizes at lower temperature than Pa. Quantifying  $^{231}\text{Pa}$  by ICP/MS thus requires that the Pa fraction eluted from the last HCl(9 N)-conditioned column be free of  $^{233}\text{U}$ . This step is

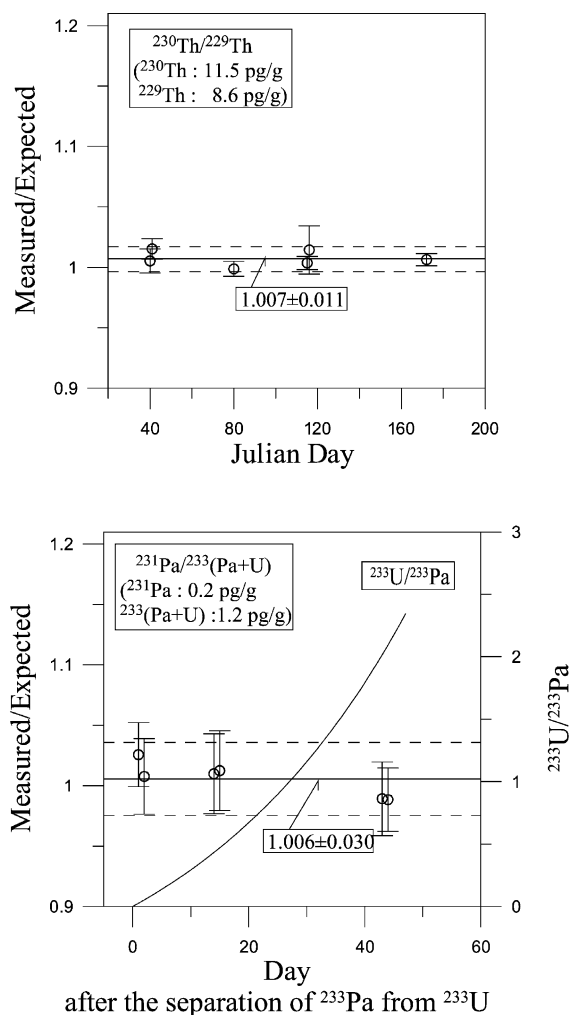


Fig. 2. Variability of isotope ratios measured on monitor solutions produced by combining calibrated Th (11.5 pg/g  $^{230}\text{Th}$  plus 8.6 pg/g  $^{229}\text{Th}$ ) and Pa (0.2 pg/g  $^{231}\text{Pa}$  plus 1.2 pg/g  $^{233}\text{Pa}$ ) standard solutions. The gradual increase in  $^{233}\text{Pa}/^{233}\text{U}$  resulting from  $^{233}\text{Pa}$  decay is also shown. Error bars represent the 95% confidence intervals.

more critical for ICP/MS measurement than for TIMS, where  $^{233}\text{U}$  can be thermally removed from the filament prior to Pa ionization. Column separation of U and Pa is very efficient, however, and can be confirmed by monitoring  $^{236}\text{U}$  (Fig. 1). If  $^{236}\text{U}$  count rates indicate significant  $^{233}\text{U}$  “bleeding” into the Pa fraction, its contribution to the 233 peak can be evaluated by eluting U from the last column and measuring its  $^{233}\text{U}/^{236}\text{U}$  ratio. Subsequent to chemi-

cal separation, the lack of differentiation between U and Pa in the plasma becomes an advantage, as samples can be then stored for at least 1 month and probably longer prior to analysis. Quantification of  $^{231}\text{Pa}$  is based on the number of atoms at mass 233 that are eluted from the last column (initially  $^{233}\text{Pa}$ , but subsequently decaying to  $^{233}\text{U}$ ). Measurements could thus be performed after the level of radioactivity in the sample has been reduced to very low levels, minimizing its impact on the detectors and complications arising from handling radioactive material.

The  $^{233}\text{Pa}$  spike is first eluted through an HCl(9 N)-conditioned column at a recorded time and subsequently calibrated against TML or a  $^{231}\text{Pa}$  standard solution (taking into account  $^{233}\text{Pa}$  decay). The calibrated spike is then added to unknown samples and the time of last elution is also recorded to calculate  $^{233}\text{Pa}$  decay between the last calibration column and the last sample column. Because  $^{233}\text{Pa}$  may be lost preferentially to  $^{233}\text{U}$  on the walls of the Teflon vials where the samples are reduced to a drop for storage before analysis, 0.3 ml of (1 N  $\text{HNO}_3$  + 0.14 N HF) is added to each sample and heated to 60 °C in a closed Teflon™ vial placed in a drying oven overnight before ICP/MS analysis to insure total solubilization of the remaining Pa.

### 3.5. Blanks and detection limits

Cumulative values from reagents to procedural blanks are reported in Table 3. All values were corrected for  $^{232}\text{Th}$  tailing and  $^{232}\text{Th}^1\text{H}$  interference. Most of  $^{230}\text{Th}$  blank ( $3.8 \pm 0.9$  fg) comes from the

Table 3  
Blank levels (fg) in the analysis of  $^{230}\text{Th}$  and  $^{231}\text{Pa}$  in seawater

Blank type	$^{230}\text{Th}$		$^{231}\text{Pa}$		$N^a$
	Mean	std <sup>b</sup>	Mean	std	
Reagent (fg) <sup>c</sup>	0.10	0.10	0.10	0.12	2
Reagent + resin (fg) <sup>c</sup>	1.11	0.34	0.19	0.08	14
Fe + reagent + resin (fg) <sup>c</sup>	4.90	0.85	0.20	0.09	2
Spike + Fe + reagent + resin (fg) <sup>d</sup>	5.79	1.08	0.63	0.13	6

<sup>a</sup>Number of measurements.

<sup>b</sup>Standard deviation.

<sup>c</sup>Calculated by external calibration.

<sup>d</sup>Calculated by isotope dilution.

Fe carrier solution, and to a lesser extent from the resin ( $\sim 1 \pm 0.4$  fg) and  $^{229}\text{Th}$  spike ( $\sim 0.9 \pm 1.4$  fg). The  $^{230}\text{Th}$  procedural blank amounts to  $\sim 15\%$  of the  $^{230}\text{Th}$  expected in  $\sim 20$  l of surface seawater (2 fg/kg). For  $^{231}\text{Pa}$ , a large fraction of the contamination ( $\sim 0.43 \pm 0.16$  fg) comes from the  $^{233}\text{Pa}$  spike.  $^{231}\text{Pa}$  is produced by neutron activation of traces of  $^{230}\text{Th}$  present in  $^{232}\text{Th}$  target used for  $^{233}\text{Pa}$  preparation (Bourdon et al., 1999). This source of contamination increases with time, as the  $^{231}\text{Pa}/^{233}\text{Pa}$  ratio of the spike increases. However, it can be precisely measured, and thus affects minimally the precision of the measurement (Table 3 indicates that the standard deviation on the blank does not increase with the spike). The Pa procedural blank amounts to  $\sim 8\%$  of the  $^{231}\text{Pa}$  present in 20 l of surface seawater (0.4 fg/kg).

Based on the standard deviation of the procedural blanks, detection limits of the method are estimated at 3.2 fg for  $^{230}\text{Th}$  and 0.4 fg for  $^{231}\text{Pa}$ , which are 5–15 times lower than the amounts found in 20 l of surface seawater.

### 3.6. Dark noise

Although the dark noise on magnetic sector ICP/MS is initially very low (typically  $< 0.3$  cps), it could increase as a result of the gradual accumulation of  $\beta$ -emitting  $^{233}\text{Pa}$  on the first dynode of the ion-counting system. After one full year of service and the analysis of nearly 300  $^{231}\text{Pa}$  samples (sediment and seawater), the dark noise of our instrument,

however, remained below 2 cps. Measurement of the instrument dark noise before and after the analysis of 13 Pa sediment samples, resulting in the introduction of  $\sim 0.1$  ng of  $^{233}\text{Pa}$  (2  $\mu\text{Ci}$ ) into the plasma, the dark noise increased from  $1.1 \pm 0.1$  to  $1.4 \pm 0.1$  (95% CI). In effect, this dark noise contributes to the “acid blanks” measured before each sample and is therefore subtracted during data reduction.

### 3.7. Data processing

Data acquisition consisted of 30 consecutive runs over the entire mass range, which averaged 30 passes each. The time-resolved raw data recorded by the ICP/MS software were exported into Excel™ spreadsheets. Count rate averages and standard deviations were calculated on the mass range corresponding to the flat top of each peak only, while the lower count rates measured on each side of the peaks were discarded. Isotopic ratios were calculated for each of the 30 consecutive runs and the reported internal precision is twice the standard deviation on the ratio divided by the square root of the number of runs. After subtraction of the column blank, the  $^{230}\text{Th}$  and  $^{231}\text{Pa}$  concentrations in the samples were calculated using standard isotope dilution equations.

### 3.8. Precision, accuracy, and sample storage

#### 3.8.1. Standard addition

Coastal seawater was filtered into 13 polyethylene cubitainers and spiked with  $^{230}\text{Th}$  and  $^{231}\text{Pa}$  to cover

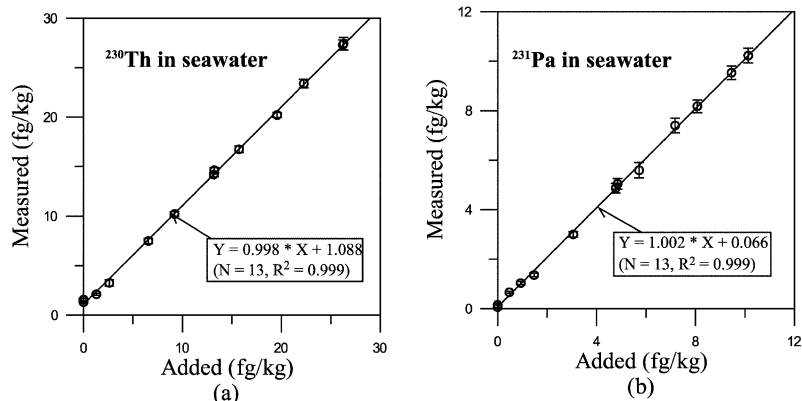


Fig. 3. Standard addition of  $^{230}\text{Th}$  (a) and  $^{231}\text{Pa}$  (b) to coastal waters and linear regression on the data.

the range of concentration found in open ocean waters ( $^{230}\text{Th}$ : 1–26 fg/kg;  $^{231}\text{Pa}$ : 0.5–10 fg/kg). Measured and added concentrations are shown in Fig. 3. The internal precision was better than 2% (2 se) for samples with concentration > 10 fg/kg and varied from 3% to 10% (2 se) at lower concentration (Table 4). The errors on intercepts indicate that the coastal seawater sample initially contained  $1.1 \pm 0.3$  fg/kg  $^{230}\text{Th}$  and  $0.07 \pm 0.11$  fg/kg  $^{231}\text{Pa}$  (95% confidence intervals (CI)). The slopes of the regressions are indistinguishable from unity ( $0.998 \pm 0.008$  for  $^{230}\text{Th}$  and  $1.002 \pm 0.009$  for  $^{231}\text{Pa}$ ). Although this is not a direct assessment of the accuracy of the measurements, since the  $^{231}\text{Pa}$  and  $^{230}\text{Th}$  standards that were used to spike the coastal seawater were calibrated against the same  $^{229}\text{Th}$  and  $^{233}\text{Pa}$  solution used for isotope dilution, the accuracy of the latter two solutions was estimated by analyzing TML to be within 1%.

### 3.8.2. Replicate analyses

The reproducibility of the analysis was tested with four sets of five replicate seawater samples (Table 5). The two sets taken from station J at 2000 m depth were immediately filtered into polyethylene cubitainers. One set was spiked and acidified as described

above. The second set was stored for a period of ~ 15 months before acidification, spiking, equilibration (for an entire week) and analysis. The results obtained on the shipboard-processed samples (Table 5) indicate an overall reproducibility (two standard deviations) of 5.2% for  $^{230}\text{Th}$  and 5.8% for  $^{231}\text{Pa}$ , which is about twice the internal precision. The unacidified samples show a clear indication of Pa loss during storage and lower reproducibility. For  $^{230}\text{Th}$ , only one of the replicate samples shows a significant loss.

The two additional sets of five replicates taken from station M, one from the mixed layer (30 m) and the other from a depth of 1500 m, were both acidified immediately after collection without filtration and stored for approximately 15 months before spiking, equilibration and analysis. Reproducibility ranged from 12.5% (two standard deviations) at concentrations < 1 fg/kg to 8.3% at higher concentration (Table 5). Reproducibility appears to be somewhat worse for unfiltered samples, possibly reflecting heterogeneity in the distribution of suspended particles. The generally lower reproducibility obtained on samples acidified but not spiked on board suggests possible erratic loss of Th during the 15-month storage. One replicate sample was also taken at 1500 m and stored without acidification. Results from this sample confirm the hydrolytic loss of both Th and Pa during storage under these conditions. These results thus indicate that the samples should be acidified as soon as possible after collection. It is also advisable that they be spiked as soon as possible, until further tests are conducted.

Table 4  
Standard addition results for  $^{230}\text{Th}$  (fg/kg) and  $^{231}\text{Pa}$  (fg/kg) in seawater

Sample no.	$^{230}\text{Th}$ (fg/kg)			$^{231}\text{Pa}$ (fg/kg)		
	Added	Measured		Added	Measured	
		Mean	2 se <sup>a</sup>		Mean	2 se
1	0	1.56	0.11	0	0.15	0.01
2	0	1.32	0.06	0	0.06	0.004
3	1.29	2.11	0.10	0.47	0.66	0.04
4	2.60	3.26	0.33	0.93	1.03	0.06
5	6.55	7.49	0.25	1.47	1.36	0.07
6	9.19	10.23	0.22	3.06	3.00	0.11
7	13.21	14.64	0.26	4.77	4.87	0.20
8	13.16	14.19	0.22	4.85	5.04	0.22
9	15.72	16.75	0.35	5.72	5.59	0.31
10	19.57	20.21	0.26	7.18	7.40	0.29
11	22.27	23.39	0.42	8.07	8.18	0.26
12	26.22	27.32	0.50	9.46	9.53	0.27
13	26.29	27.43	0.63	10.13	10.23	0.30

<sup>a</sup>Internal precision (95% confidence level).

### 3.9. Water column profiles

“Oceanographic consistency” provides another means of assessing the quality of our measurements. Deep-water circulation has a predictable effect on  $^{230}\text{Th}$  and  $^{231}\text{Pa}$  seawater profiles. When water circulation is neglected, a reversible scavenging model predicts linear increases in the concentration of both radionuclides with depth (Bacon and Anderson, 1982). Deep-water formation in the North Atlantic thus decreases deep water concentration, which gradually increases as the newly formed deep water ages and regains steady-state with respect to scavenging

Table 5  
 Reproducibility and storage effects in the analysis of  $^{230}\text{Th}$  and  $^{231}\text{Pa}$  in seawaters

	$^{230}\text{Th}$ (fg/kg)						$^{231}\text{Pa}$ (fg/kg)											
	St. M, 30 m (unfiltered)			St. M, 1500 m (unfiltered)			St. J, 2000 m (filtered)			St. M, 30 m (unfiltered)			St. M, 1500 m (unfiltered)			St. J, 2000 m (filtered)		
	Sample	Mean	2 se	Sample	Mean	2 se	Sample	Mean	2 se	Sample	Mean	2 se	Sample	Mean	2 se	Sample	Mean	2 se
On board acidified <sup>a</sup> and spiked							15 and 16	9.05	0.1							15 and 16	3.64	0.16
							17 and 18	9.17	0.1							17 and 18	3.55	0.18
							19 and 20	9.29	0.2							19 and 20	3.76	0.25
							21 and 22	9.62	0.2							21 and 22	–	
							23 and 24	9.52	0.2							23 and 24	–	
							Mean	9.33								Mean	3.65	
						std	0.24								std	0.11		
Acidified on board and stored (15 months)	1 and 2 <sup>b</sup>	2.88	0.1	1 and 2	8.15	0.15				1 and 2	0.42	0.07	1 and 2	3.71	0.14			
	3 and 4	3.07	0.11	3 and 4	8.54	0.13				3 and 4	0.5	0.04	3 and 4	3.54	0.13			
	5 and 6	2.81	0.09	5 and 6	8.61	0.17				5 and 6	0.46	0.05	5 and 6	3.64	0.15			
	7 and 8	– <sup>c</sup>		7 and 8	9.07	0.19				7 and 8	0.45	0.04	7 and 8	3.96	0.18			
	9 and 10	3.09	0.09	9 and 10	8.11	0.18				9 and 10	0.45	0.05	9 and 10	3.71	0.18			
	Mean	2.96		Mean	8.49					Mean	0.46		Mean	3.71				
std <sup>d</sup>	0.14		std	0.39					std	0.03		std	0.15					
Unacidified and stored (15 months)							5 and 6	7.27	0.19						5 and 6	2.09	0.18	
							7 and 8	9.27	0.22						7 and 8	1.92	0.2	
				11 and 12	6.87		9 and 10	–				11 and 12	2.52		9 and 10	2.68	0.21	
							11 and 12	9.11	0.18						11 and 12	2.46	0.27	
							13 and 14	9.27	0.19						13 and 14	2.28	0.18	
							Mean	8.73							Mean	2.29		
							std	0.97							std	0.3		

<sup>a</sup>30 ml of 6 N HCl into 20 l seawater.

<sup>b</sup>Bottle number on rosette.

<sup>c</sup>Samples lost during measurements.

<sup>d</sup>Standard deviation.

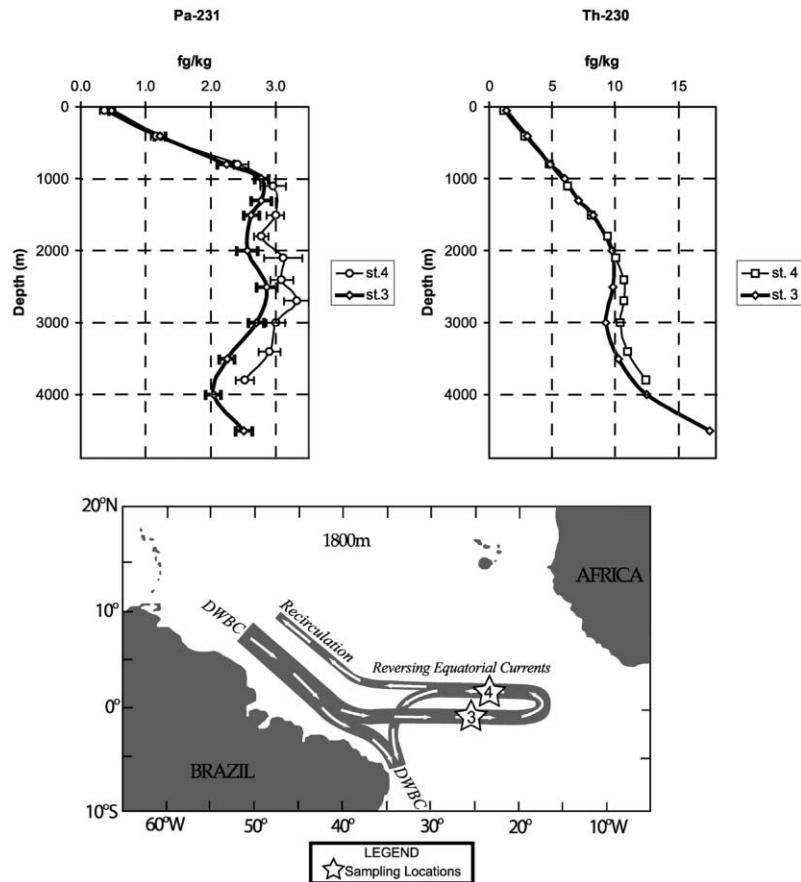


Fig. 4. Dissolved  $^{231}\text{Pa}$  and  $^{230}\text{Th}$  profiles at two stations in the equatorial Atlantic showing the gradual ingrowth of the two nuclides in deep water between Stations 3 and 4. Error bars for  $^{231}\text{Pa}$  represent internal precision at the 95% confidence interval. Same error bars for  $^{230}\text{Th}$  are within the symbols used to represent the data. Schematic of the Deep Western Boundary Current (DWBC) is from Schmitz (1996).

(Rutgers van der Loeff and Berger, 1993; Moran et al., 1997; Francois et al., 2000). This effect can be clearly discerned in two profiles of dissolved  $^{230}\text{Th}$  and  $^{231}\text{Pa}$  taken in the equatorial recirculation loop of the Deep Western Boundary Current (DWBC). Station 3 sampled the younger water in the eastward branch of the loop. Station 4 sampled the older water in the westward branch (Fig. 4). The profiles overlap in the upper 1000 m for  $^{231}\text{Pa}$  and the upper 2000 m for  $^{230}\text{Th}$ , where steady state with respect to scavenging has already been regained. In deeper water, however, both nuclides show measurable increases in concentration between the two stations that can be

used to constrain deep water circulation and mixing rates (Francois et al., 2000).

### Acknowledgements

This work was funded by the National Science Foundation (OCE-9415562 to MPB and RF; OCE-9730967 to KWS), and benefited from the use of the MIT Nuclear Reactor Laboratory supported by US DOE Reactor sharing grant N0 DE-FG07-80ER-10770-A20. This work was also supported by a KOSEF post-doctoral fellowship to M.S. Choi and a

WHOI post-doctoral fellowship to K. Sims. The authors acknowledge the careful reviews of G. Henderson and two anonymous referees. The measurements were made in the WHOI ICP/MS facility. This is WHOI contribution 10448.

## References

- Anderson, R.F., Fleer, A.P., 1982. Determination of natural actinides and plutonium in marine particulate material. *Anal. Chem.* 54, 1142–1147.
- Bacon, M.P., 1984. Glacial to interglacial changes in carbonate and clay sedimentation in the Atlantic Ocean estimated from  $^{230}\text{Th}$  measurements. *Isot. Geosci.* 2, 97–111.
- Bacon, M.P., 1988. Tracers of chemical scavenging in the ocean: boundary effects and large scale chemical fractionation. *Philos. Trans. R. Soc. London, Ser. A* 325, 147–160.
- Bacon, M.P., Anderson, R.F., 1982. Distribution of thorium isotopes between dissolved and particulate forms in the deep sea. *J. Geophys. Res.* 87, 2045–2056.
- Becker, J.S., Soman, S.V., Sutton, K.L., Caruso, J.A., Dietze, H.-J., 1999. Determination of long-lived radionuclides by inductively coupled plasma quadrupole mass spectrometry using different nebulizers. *J. Anal. At. Spectrom.* 14, 933–937.
- Bourdon, B., Joron, J.-L., Allègre, C.J., 1999. A method for  $^{231}\text{Pa}$  analysis by thermal ionization mass spectrometry in silicate rocks. *Chem. Geol.* 157, 147–151.
- Buesseler, K.O., Cochran, J.K., Bacon, M.P., Livingston, H.D., Casso, S.A., Hirschberg, D., Hartman, M.C., Fleer, A.P., 1992. Determination of thorium isotopes in seawater by non-destructive and radiochemical procedures. *Deep-Sea Res.* 39, 1103–1114.
- Catterick, T., Fairman, B., Harrington, C., 1998. Structured approach to achieving high accuracy measurements with isotope dilution inductively coupled plasma mass spectrometry. *J. Anal. At. Spectrom.* 13, 1009–1013.
- Cochran, J.K., 1992. The oceanic chemistry of the uranium- and thorium-series nuclides. In: Ivanovich, M., Harmon, R.S. (Eds.), *Uranium-Series Disequilibrium: Applications to Earth, Marine, and Environmental Sciences*. Clarendon Press, Oxford, pp. 334–395.
- Crain, J., Alvarado, J., 1994. Hydride interference on the determination of minor actinide isotopes by inductively coupled plasma mass spectrometry. *J. Anal. At. Spectrom.* 9, 1223–1227.
- Edmonds, H.N., Moran, S.B., Hoff, J.A., Smith, J.N., Edwards, R.L., 1998. Protactinium-231 and thorium-230 abundances and high scavenging rates in the western Arctic Ocean. *Science* 280, 405–407.
- Eroglu, A.E., McLeod, C.W., Leonard, K.S., McCubbin, D., 1998. Determination of plutonium in seawater using co-precipitation and inductively coupled plasma mass spectrometry with ultrasonic nebulization. *Spectrochim. Acta, Part B* 53, 1221–1233.
- Field, M.P., Sherrell, R.M., 1998. Magnetic sector ICPMS with desolvating micronebulization: interference-free subpicogram determination of rare earth elements in natural samples. *Anal. Chem.* 70, 4480–4486.
- Fleer, A.P., Bacon, M.P., 1991. Notes on some techniques of marine particle analysis used at WHOI. In: Hurd, D.C., Spencer, D.W. (Eds.), *Marine Particles: Analysis and Characterization*. Geophys. Monogr., vol. 63, AGU, Washington, D.C., pp. 223–226.
- Francois, R., Bacon, M.P., Suman, D.O., 1990. Thorium-230 profiling in deep-sea sediments: high-resolution records of flux and dissolution of carbonate in the equatorial Atlantic during the last 24,000 years. *Paleoceanography* 5, 761–787.
- Francois, R., Bacon, M.P., Altabet, M.A., Labeyrie, L.D., 1993. Glacial/interglacial changes in sediment rain rate in the SW Indian sector of subantarctic waters as recorded by  $^{230}\text{Th}$ ,  $^{231}\text{Pa}$ , U and  $\delta^{15}\text{N}$ . *Paleoceanography* 8, 611–629.
- Francois, R., Altabet, M.A., Yu, E.F., Sigman, D.M., Bacon, M.P., Frank, M., Bohrmann, G., Bareille, G., Labeyrie, L.D., 1997. Contribution of Southern Ocean upper water column stratification to the glacial decrease in atmospheric  $\text{CO}_2$ . *Nature* 389, 929–935.
- Francois, R., Bacon, M.P., Bullister, J., Fleer, A.P., Brown-Leger, S., Wisegarver, D., 2000. Constraining deep water circulation and mixing in the Atlantic from  $^{230}\text{Th}$  and  $^{231}\text{Pa}$  seawater profiles. *Ocean Science Meeting Abstract*, San Antonio.
- Frank, M., Gersonde, R., Mangini, A., 1999. Sediment redistribution,  $^{230}\text{Th}_{\text{ex}}$ -normalization and implication for the reconstruction of particle flux and export paleoceanography. In: Fischer, G., Wefer, G. (Eds.), *Use of Proxies in Paleoceanography: Examples from the South Atlantic*. Springer-Verlag, Berlin, pp. 409–426.
- Hallenbach, M., Grohs, J., Mamich, S., Kroft, M., 1994. Determination of technetium-99, thorium-230 and uranium-234 in soils by inductively coupled plasma mass spectrometry using flow injection preconcentration. *J. Anal. At. Spectrom.* 9, 927–933.
- Henderson, G.M., Heinze, C., Anderson, R.F., Winguth, A.M.E., 1999. Global distribution of the  $^{230}\text{Th}$  flux to ocean sediments constrained by GCM modeling. *Deep-Sea Res., Part I* 46, 1861–1893.
- Heumann, K.G., Gallus, S.M., Radlinger, G., Vogl, J., 1998. Precision and accuracy in isotope ratio measurements by plasma source mass spectrometry. *J. Anal. At. Spectrom.* 13, 1001–1008.
- Hinrichs, J., Schnetger, B., 1999. A fast method for the simultaneous determination of  $^{230}\text{Th}$ ,  $^{234}\text{U}$  and  $^{235}\text{U}$  with isotope dilution sector field ICP-MS. *Analyst* 124, 927–932.
- Kim, C.-S., Kim, C.-K., Lee, J.-I., Lee, K.-J., 2000. Rapid determination of Pu isotopes and atom ratios in small amounts of environmental samples by an on-line pre-treatment system and isotope dilution high resolution inductively coupled plasma mass spectrometry. *J. Anal. At. Spectrom.* 15, 247–255.
- Kumar, N., Gwiazda, R., Anderson, R.F., Froelich, P.N., 1993.  $^{231}\text{Pa}/^{230}\text{Th}$  ratios in sediments as a proxy for past changes in Southern Ocean productivity. *Nature* 362, 45–48.
- Lao, Y., Anderson, R.F., Broecker, W.S., Trumbore, S.E., Hoffmann, H.J., Wolfi, W., 1992. Transport and burial rates of

- $^{10}\text{Be}$  and  $^{231}\text{Pa}$  in the Pacific Ocean during Holocene period. *Earth Planet. Sci. Lett.* 113, 173–189.
- Layne, G.D., Sims, K.W., 2000. Analysis of  $^{232}\text{Th}/^{230}\text{Th}$  in volcanic rocks by Secondary Ionization Mass Spectrometry. *Int. J. Mass Spectrom.* 203, 187–198.
- Luo, S., Ku, T.-L., Kusakabe, M., Bishop, J.K.B., Yang, Y.-L., 1995. Tracing particle cycling in the upper ocean with  $^{230}\text{Th}$  and  $^{228}\text{Th}$ : an investigation in the equatorial Pacific along  $140^\circ\text{W}$ . *Deep-Sea Res., Part II* 42, 805–829.
- Marchal, O., Francois, R., Stocker, T.F., Joos, F., 2000. Ocean thermohaline circulation and sedimentary  $^{231}\text{Pa}/^{230}\text{Th}$  ratio. *Paleoceanography* 15, 625–641.
- Minnich, M.G., Houk, R.S., 1998. Comparison of cryogenic and membrane desolvation for attenuation of oxide, hydride and hydroxide ions and ions containing chlorine in inductively coupled plasma mass spectrometry. *J. Anal. At. Spectrom.* 13, 167–174.
- Moran, S.B., Hoff, J.A., Buesseler, K.O., Edwards, R.L., 1995. High precision  $^{230}\text{Th}$  and  $^{232}\text{Th}$  in the Norwegian Sea and Denmark by thermal ionization mass spectrometry. *Geophys. Res. Lett.* 22, 2589–2592.
- Moran, S.B., Charette, M.A., Hoff, J.A., Edwards, R.L., Landing, W.M., 1997. Distribution of  $^{230}\text{Th}$  in the Labrador Sea and its relation to ventilation. *Earth Planet. Sci. Lett.* 150, 151–160.
- Nozaki, Y., Nakanishi, T., 1985.  $^{231}\text{Pa}$  and  $^{230}\text{Th}$  profiles in the open ocean water column. *Deep-Sea Res.* 32, 1209–1220.
- Nozaki, Y., Horibe, Y., Tsubota, H., 1981. The water column distributions of thorium isotopes in the western North Pacific. *Earth Planet. Sci. Lett.* 54, 203–216.
- Nozaki, Y., Yang, H.-S., Yamada, M., 1987. Scavenging of thorium in the ocean. *J. Geophys. Res.* 92, 772–778.
- Pickett, D.A., Murrell, M.T., Williams, R.W., 1994. Determination of femtogram quantities of protactinium in geologic samples by thermal ionization mass spectrometry. *Anal. Chem.* 66, 1044–1049.
- Rutgers van der Loeff, M.M., Berger, G.W., 1993. Scavenging of  $^{230}\text{Th}$  and  $^{231}\text{Pa}$  near the Antarctic Polar Front on the South Atlantic. *Deep-Sea Res.* 40, 339–357.
- Schmitz, W.J., Jr., 1996. On the World Ocean Circulation, vol. 1. Woods Hole Oceanographic Institution Technical Report (WHOI-96-03).
- Scholten, J.C., Rutgers van der Loeff, M.M., Michel, A., 1995. Distribution of  $^{230}\text{Th}$  and  $^{231}\text{Pa}$  in the water column in relation to the ventilation of the deep Arctic basins. *Deep-Sea Res.* 42, 1519–1531.
- Shaw, T.J., Francois, R., 1991. A fast and sensitive ICP–MS assay for the determination of  $^{230}\text{Th}$  in marine sediments. *Geochim. Cosmochim. Acta* 55, 2075–2078.
- Sims, K.W.W., Goldstein, S.J., Blichert-Toft, J., Perfit, M.R., Kelemen, P., Fornari, D.J., Michael, P., Murrell, M.P., Hart, S.R., DePaolo, D.J., Layne, G., Jull, M., submitted for publication. Chemical and isotopic constraints on the generation and transport of melt beneath the East Pacific Rise. *J. Geophys. Res.*
- Suman, D.O., Bacon, M.P., 1989. Variations in Holocene sedimentation in the north American basin determined from Th-230 measurements. *Deep-Sea Res.* 36, 869–878.
- Vogler, S., Scholten, J., Rutgers van der Loeff, M.M., Mangini, A., 1998.  $^{230}\text{Th}$  in the eastern North Atlantic: the importance of water mass ventilation in the balance of  $^{230}\text{Th}$ . *Earth Planet. Sci. Lett.* 156, 61–74.
- Walter, H.-J., Rutgers van der Loeff, M.M., Francois, R., 1999. Reliability of the  $^{231}\text{Pa}/^{230}\text{Th}$  activity ratio as a tracer for bioproductivity of the ocean. In: Fischer, G., Wefer, G. (Eds.), *Use of Proxies in Paleoceanography: Examples from the South Atlantic*. Springer-Verlag, Berlin, pp. 393–408.
- Yu, E.-F., Francois, R., Bacon, M.P., 1996. Similar rates of modern and last-glacial ocean thermohaline circulation inferred from radiochemical data. *Nature* 379, 689–694.